27th ABCM International Congress of Mechanical Engineering
December 04-08, 2023, Florianópolis-SC, Brazil

COB-2023-1816
Estimation of boundary heat flux in Micro-Channels Via Bayesian Inference By The Transitional Markov Chain Monte Carlo Algorithm

Lucas da Silva Asth
lucas.asth@iprj.uerj.br
Luiz A. S. Abreu
luiz.abreu@iprj.uerj.br
Diego Campos Knupp
diegoknupp@iprj.uerj.br
Leonardo Tavarez Stutz
ltstutz@iprj.uerj.br
Eduardo Cunha Classe
eduardo.classe@iprj.uerj.br

Universidade do Estado do Rio de Janeiro - Instituto Politécnico
Rua Bonfim Vila Amélia, Nova Friburgo, RJ - Brasil.

Abstract. *The estimation of heat fluxes at the boundary of micro-channels has great interest in many engineering applications as in micro-electromechanical systems or in thermal control of microelectronics. However, in cases where direct temperature measurements cannot be taken, this information can still be obtained through the application of an inverse problems approach. Inverse problems related to micro-scale heat transfer and microfluidics have become more widely studied in recent decades due to advances in technology. This work deals with a Bayesian inverse problem of boundary heat flux profile in a micro-channel under slip-flow conditions using the Transitional Markov Chain Monte Carlo method. The boundary heat flux profile is estimated based on non-intrusive temperature measurements supposedly taken with a thermographic camera. The direct problem was solved using the finite element method implemented by the NDSolve function, which is an intrinsic function of Mathematica Software. The Transitional Markov Chain Monte Carlo Method algorithm was used to solve the inverse problem due to its advantages over the classic Markov Chain Monte Carlo Method. Bayesian methods have become increasingly popular in inverse analysis due to their ability to incorporate prior information and quantify uncertainties. The Transitional Markov Chain Monte Carlo Method is a more recent Bayesian algorithm that has several advantages. It is a tune-free algorithm, meaning it does not require the specification of a proposal probability density function, and it can estimate the model evidence and make model comparisons without extra computation costs. The proposed methodology was analyzed by simulated temperature measurements with different boundary heat flux function shapes, revealing the capability of the approach, even in discontinuous functions. The proposed methodology provides a way to obtain statistical uncertainties based on temperature measurements, making it a valuable tool in the design and optimization of micro-channel heat transfer systems.*

Keywords: *Bayesian Inference, Heat Transfer, Inverse Problems, Microchannel, Transitional Markov Chain Monte Carlo*

1. INTRODUCTION

The rapid progress in the technological advancements of microprocessors and integrated circuits has significantly increased data processing capabilities while reducing the physical size of devices. Consequently, this has led to a higher heat generation, primarily due to the Joule Effect, resulting in elevated component temperatures. Such temperature rise poses a risk of increased system failures and reduced overall lifespan (Mercone *et al.*, 2005), thereby necessitating effective thermal management strategies for these devices.

One promising solution that is currently being developed is liquid cooling, which aims to enhance heat transfer through convective mechanisms by circulating a refrigerant fluid within microchannels (Tuckerman and Pease, 1981; Yarin *et al.*, 2009; Cotta *et al.*, 2016). Tuckerman and Pease successfully demonstrated the practical implementation of miniaturized cooling devices for high-heat-generating electronics, utilizing water as the refrigerant within a microchannel-based heat sink (Tuckerman and Pease, 1981). The utilization of mini and microchannels offers a significantly larger heat transfer area relative to the fluid volume, resulting in more efficient heat dissipation when compared to conventional macro-scale systems (Chen *et al.*, 2022).

In situations involving Heat Transfer, direct problems aim to determine the distribution of temperatures over time, given knowledge of the physical properties, boundary and initial conditions, and the geometry in question. On the other hand, inverse problems involve determining the properties involved in the formulation of the problem, such as thermal conductivity, heat flux, convective heat transfer coefficient, geometry, boundary conditions, among others, given knowledge of the temperature field. In short, the direct problem determines the effects given the causes, while the inverse problem determines the causes given the effects (Orlande, 2015; Ozisik and Orlande, 2021; Kaipio and Somersalo, 2006).

This work aims to estimate the heat flux positioned on one of the boundaries of a microchannel, simulating the heat generation given by a processor. The mathematical model used incorporates slip-flow conditions, which are characteristic of microscale flows. The inverse problem was solved using the Transitional Markov Chain Monte Carlo Method, which offers some advantages such as its tune-free characteristics, meaning it does not require the specification of a proposal probability density function, and it can estimate the model evidence and make model comparisons without additional computational costs.

2. CONVECTIVE HEAT TRANSFER IN MICRO-CHANNELS

The inverse problem of heat flux estimation requires first a solution to the direct problem of forced convection in micro-channels. A numerical solution to the direct problem is only possible once boundary conditions are specified, which includes the boundary heat flux. In a Transitional Markov Chain Monte Carlo method, the direct problem must be solved multiple times as the parameters to be estimated are treated as independent random variables (Orlande (2015)). Simulated measurements taken at the upper surface of the microchannel are used for the inverse solution.

2.1 Direct Problem

The direct problem consists of a microscale forced convection phenomenon between parallel plates within the slip-flow regime (Kandlikar *et al.*, 2005). The model is based on a steady laminar gas flow under thermal development and a fully developed velocity profile at the inlet. The fluid exchanges heat by convection with the walls, which have length b and d is the distance between them. The problem is in a steady-state with temperature varying in a bi-dimensional space. The effects of axial conduction, free convection and viscous dissipation are neglected and physical properties are assumed constant. Figure 1 illustrates a schematic representation of the physical problem at hand.

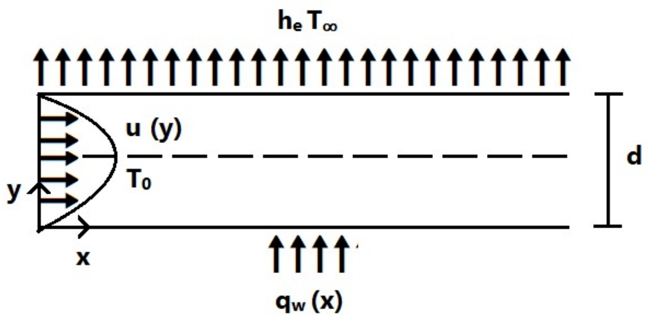

Figure 1. Schematic representation of the physical problem

The dimensionless formulation that models the heat transfer phenomenon in question is as follows:

$$\frac{\partial^2\Theta(X,Y)}{\partial Y^2} = U(Y)\frac{\partial\Theta(X,Y)}{\partial X} \qquad \text{at,} \quad 0 < Y < 1, \;\; 0 < X < L \tag{1}$$

$$\frac{\partial\Theta(X,Y)}{\partial X} = \frac{B_i}{1 + K_n\beta_t B_i}\Theta(X,Y) \qquad \text{at,} \quad Y = 1, \;\; 0 < X \tag{2}$$

$$\frac{\partial\Theta(X,Y)}{\partial X} = Q \qquad \text{at,} \quad Y = 1, \;\; 0 < X \tag{3}$$

$$\Theta(X,Y) = \Theta_0 \qquad \text{at,} \quad Y = 1, \;\; 0 < X \tag{4}$$

the dimensionless quantities B_i and K_n in the Eq.(2) and Eq.(13) are the Biot and Knudsen numbers respectively, with their characteristic lengths being equal to d, the distance between the walls. The quantities, β_t, the temperature jump coefficient and β_v, the velocity slip coefficient, are related to the loss of adherence to the wall. The dimensionless groups are:

$$X = \frac{\alpha x}{u_m d^2} \tag{5}$$

$$Y = \frac{y}{d} \tag{6}$$

$$Q = \frac{d}{k\Delta T_0} q_w \tag{7}$$

$$\Theta(X,Y) = \frac{T(x,y) - T_\infty}{T_0 - T_\infty} \tag{8}$$

$$B_i = \frac{h_e d}{k} \tag{9}$$

$$K_n = \frac{\lambda}{2d} \tag{10}$$

$$U(Y) = \frac{u(y)}{u_m} \tag{11}$$

and,

$$\beta_t = \frac{(2-\alpha_t)}{\alpha_t} \frac{2\gamma}{(\gamma+1)} \frac{1}{P_r} \tag{12}$$

is the wall temperature jump coefficient and α_t is the thermal accommodation coefficient, λ is the molecular mean free path, $\gamma = c_p/c_v$, while c_p is specific heat at constant pressure, c_v specific heat at constant volume and P_r is the Prandtl number. ecific heat at constant volume and Pr is the Prandtl number. The dimensionless velocity profile is given as (Cotta *et al.*, 2016)

$$U(Y) = \frac{6K_n\beta_v + 6Y(1-Y)}{1 + 6K_n\beta_v} \tag{13}$$

where,

$$\beta_v = \frac{(2-\alpha_m)}{\alpha_m} \tag{14}$$

is the wall velocity slip coefficient and α_m is the tangential momentum accommodation coefficient. In these dimensionless groups, α is the thermal diffusivity, u_m is the mean velocity, T is temperature of the fluid and q_w is the heat flux imposed at the boundary. The solution to this proposed problem is achieved by a computational routine in the Wolfram Mathematica platform, using a NDSolve tool which is a numerical solver for differential equations.

2.2 Inverse Problem

The inverse problem aims to estimate the boundary heat flux through Bayesian inference. This approach consists of using available prior information in order to reduce uncertainty in decision-making problems. To combine new information with all prior information, we use Bayes' theorem Eq. (15) to form the basis of statistical processes.

$$p(\theta|\mathbf{d}) = \frac{p(\theta)p(\mathbf{d}|\theta)}{p(\mathbf{d})} \tag{15}$$

$p(\theta|\mathbf{d})$ is the posterior probability density, which is the conditional density of the parameters P given the measurements $\mathbf{d}$; $p(\theta)$ is the prior density of the parameters, that is, the available information for the parameters before the measurements are taken; $p(\mathbf{d}|\theta)$ is the likelihood function, which expresses the probability density of the measurements $\mathbf{d}$ given the parameters θ, and $(\mathbf{d})$ is the marginal density of probability of the measurements, essentially playing the role of a normalization constant.

Considering measurement errors as additive and independent of the parameters θ, and following a Gaussian probability distribution with zero mean and known covariance matrix $\mathbf{W}$, the likelihood function can be represented as described by (Kaipio and Somersalo, 2006).

$$p(\mathbf{d}|\theta) = \frac{1}{\sqrt{(2\pi)^{N_d}}} |\mathbf{W}|^{-\frac{1}{2}} \cdot \exp\left(-\frac{1}{2}[\mathbf{d} - T(\theta)]^T \mathbf{W}^{-1} [\mathbf{d} - T(\theta)]\right) \tag{16}$$

2.2.1 Transitional Markov Chain Monte Carlo

The TMCMC method starts with independent samples from a prior distribution. In the subsequent steps, the sampling distribution is gradually transformed to approximate the posterior distribution. Thus, the equation of Bayes' theorem (15) is modified as follows:

$$p_j(\boldsymbol{\theta}) \propto p(\boldsymbol{\theta}) \cdot L(\boldsymbol{\theta}|\mathbf{d})^{q_j} \tag{17}$$

Here, $j = 0, \ldots, m$ denotes the stage of transition, and $q_j \in [0, 1]$ is chosen such that $q_0 = 0 < q_1 < \cdots < q_m = 1$. Consequently, for $j = 0$, $p_0(\boldsymbol{\theta})$ is the prior distribution $p(\boldsymbol{\theta})$, and for $j = m$, $p_m(\boldsymbol{\theta})$ becomes the posterior distribution $p(\boldsymbol{\theta}|\mathbf{d})$. Thus, the TMCMC method gradually pushes the samples from prior to posterior through a transition of distributions (Betz *et al.*, 2016). The speed of this transition is controlled by the coefficient q_j. In (Ching and Chen, 2007), it was proposed to select q_j such that the coefficient of variation of $L(\boldsymbol{\theta}|\mathbf{d})^{q_{j+1}-q_j}$ is approximately equal to v_t, where $v_t = 100\%$ is suggested. The value of q_{j+1} can be determined based on the samples from the previous stage using:

$$q_{j+1} = \text{argmin}(|CV_j(q) - v_t|) \tag{18}$$

$CV_j(q)$ is the coefficient of variation of the set $\left\{L(\boldsymbol{\theta}_{j,k}|\mathbf{d})^{q-qj}\right\}_{k=1}^{Ns}$, N_s is the number of samples generated at each stage, $\boldsymbol{\theta}_{j,k}$ denotes the k-th sample in stage j, and $L(\boldsymbol{\theta}_{j,k}|\mathbf{d})$ is the likelihood associated with $\boldsymbol{\theta}_{j,k}$.

The TMCMC algorithm can be summarized as follows: For $j = 0$, all N_s samples are drawn from the prior distribution, and j is then set to 1. For all $j > 0$, the scheme used in this work will be based on the improved algorithm proposed in (Betz *et al.*, 2016).

1. Find the value of q_j using (Eq. 18). If $q_j > 1$, then set $q_j = 1$.
2. For all samples $k = 1, \ldots, N_s$, calculate the weighted coefficients $w_{(j,k)}$:
$$w_{(j,k)} = (L(\boldsymbol{\theta}_{j-1,k}|\mathbf{d}))^{q_j - q_{j-1}} \tag{19}$$
3. Calculate the mean of the weighted coefficients:
$$S_j = \frac{1}{N_s}\sum_{k=1}^{N_s} w_{(j,k)} \tag{20}$$
4. Calculate the covariance matrix of the proposed Gaussian distribution:
$$\boldsymbol{\Sigma}_j = \beta^2 \cdot \sum_{k=1}^{N_s}\left[\frac{w_{(j,k)}}{S_j \cdot N_s} \cdot (\boldsymbol{\theta}_{(j-1,k)} - \bar{\boldsymbol{\theta}}_j) \cdot (\boldsymbol{\theta}_{(j-1,k)} - \bar{\boldsymbol{\theta}}_j)^T\right] \tag{21}$$
where
$$\bar{\boldsymbol{\theta}}_j = \frac{\sum_{l=1}^{N_s} w_{(j,l)} \cdot \boldsymbol{\theta}_{(j-1,l)}}{\sum_{l=1}^{N_s} w_{(j,l)}} \tag{22}$$
The coefficient β scales the proposed distribution. (Betz *et al.*, 2016) suggest an initial value of $\beta_{old} = 2.4/\sqrt{M}$, where M is the number of parameters in the vector $\boldsymbol{\theta}$.
5. For each l in $1, \ldots, N_s$, do: $\boldsymbol{\theta}^c_{(j,l)} = \boldsymbol{\theta}_{(j-1,l)}$. After that, for $k = 1, \ldots, N_s$:
   - Set $w_{(j,l)} = L(\boldsymbol{\theta}^c_{(j,l)}|\mathbf{d})^{qj - q_{j-1}}$.
6. The value of β is then chosen adaptively:
   - At the beginning of each sampling stage, set $N_{adapt} = 1$; Perform N_a steps of MCMC.
   - Evaluate the coefficient $c_a = (p_{acr} - t_{acr})/\sqrt{N_{adapt}}$, where p_{acr} is the average acceptance rate over the last N_a steps of MCMC, and t_{acr} is the target acceptance rate.

- Modify β based on the value of c_a. Set $\beta_{new} = \beta_{old} \cdot \exp(c_a)$.
- Increase the value of N_{adapt} by 1 and set $\beta_{old} = \beta_{new}$.
- Repeat the procedure until the desired number of samples is generated.

A value of $N_a = 100$ is suggested (Betz *et al.*, 2016).

7. If $q_j = 1$, then stop the iteration; otherwise, set $j = j + 1$ and continue with step 1.

3. RESULTS AND DISCUSSION

In order to generate the following results a computational routine was developed in the Wolfram Mathematica platform. The direct problem is solved by using the NDSolve function, which is a differential equations solver, built-in the software and the inverse solution followed the Transitional Markov Chain Monte Carlo algorithm. Values used for the micro fluid flow dimensionless properties and geometry were taken from the work of (Naveira-Cotta *et al.*, 2010). The following values were adopted $\beta_v = 1.5$, $\beta_t = 2.0$, $K_n = 0.025$, $B_i = 2.0$ and $L = 1.25$. The experimental data is comprised of two hundred temperature measurements taken at position $Y = 1.0$ which is the upper surface of the microchannel. The measurements are simulated as normal distributions with averages at their exact values and 0.1^{o}C standard deviation. The parameters used in the TMCMC were: $N_s = 5000$ samples, $\beta = 0.2$, and $COV = 100\%$

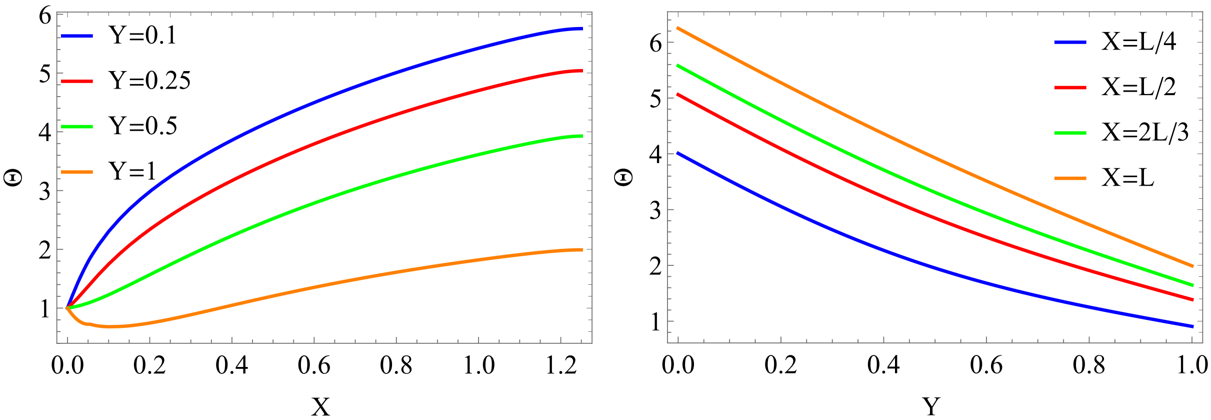

Figure 2. Solution of the direct problem

Figure 2 shows the solution of the forward problem along the X and Y axes for different positions of the domain. For heat flux estimation, three distinct models were considered: (1) Constant heat flux; (2) Linear spatially varying heat flux; (3) Quadratic spatially varying heat flux. It is worth noting that for the cases with spatially varying heat flux, the parameters to be estimated are the coefficients that constitute the function. The different proposed models are represented in the Table 1

Table 1. models considered for the heat flux Q.

Model	Description	Vector of uncertain parameters
$\mathcal{M}_0$	$Q(x) = c$	$\boldsymbol{\theta} = [c]^T$
$\mathcal{M}_1$	$Q(x) = bx + c$	$\boldsymbol{\theta} = [b, c]^T$
$\mathcal{M}_2$	$Q(x) = ax^2 + bx + c$	$\boldsymbol{\theta} = [a, b, c]^T$

In the following numerical analyses, observed data *(synthetic experimental data)* of temperature were considered, obtained from the response of a reference model with zero-mean Gaussian noise with a standard deviation of 0.1 ^{o}C. three distinct cases will be addressed. In Cases 1A, 2A, and 3A, the reference models used to generate the observed data are identical to the models considered in the inversion process, a situation commonly referred to as the *"inverse crime"*. Therefore, in these cases, the uncertain parameters of the model in the inversion process have reference values, which are the values of the parameters used in generating the observed data. The reference models, as well as the reference values of the parameters used in generating the observed data in Cases 1A, 2A, and 3A, are presented in the Table 2

3.1 Case 1A

In the first case studied, the parameter of interest, Q, is considered constant along the length of the microchannel. The prior probability density of the uncertain parameter was adopted as $Q \sim \mathcal{U}[0, 15]$, where $\mathcal{U}[u_1, u_2]$ represents a uniform

Table 2. Reference models and reference parameters for generating the data observed in Cases 1A, 2A and 3A.

Reference Models	**Reference Parameters**	**Reference Values**
$\mathcal{M}_0$	$\boldsymbol{\theta} = [c]^T$	$[5.0]^T$
$\mathcal{M}_1$	$\boldsymbol{\theta} = [b, c]^T$	$[-2.0; 5.0]^T$
$\mathcal{M}_2$	$\boldsymbol{\theta} = [a, b, c]^T$	$[-10.0; 5.0; 4.0]^T$

distribution in the interval between u_1 and u_2. Figure 3 shows the histogram of the posterior density of the samples and the plot of the evolution of the stages q_j. The algorithm took 7 stages to reach the final distribution and counting all stages, there are a total of $35,000$ samples, and only the last $5,000$ samples are actually from the posterior probability density function. Table 3 displays the inferred statistical data about the estimated parameter.

Table 3. Statistical inferences of Q, model $\mathcal{M}_0$

Exact Value	**Mean**	**Standard Deviation**
5.0	4.99798	0.03717

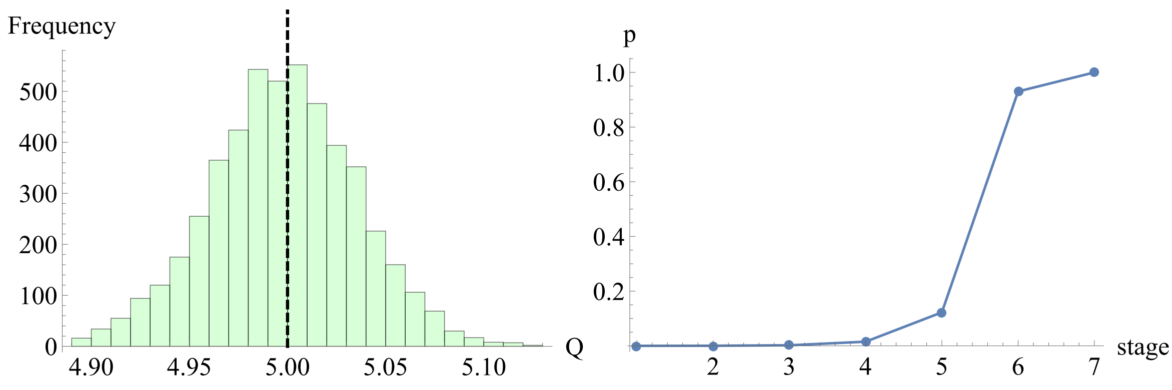

Figure 3. Histogram of the posterior and evolution of the stages, model $\mathcal{M}_0$

The forward problem was then solved again with the mean value of Q found in the inverse problem. Figure 4 shows the comparison of solutions with the exact Q and the estimated Q along the length L in the X direction as well as in the Y direction. Finally, Figure 5 shows the credibility interval of the problem's response in relation to the experimental data. It is possible to observe that the credibility interval encompasses the exact solution to the problem, but this does not happen with the experimental data with deviation. This is due to the low sensitivity of the problem to the parameter under study and also to the high experimental uncertainty used in the problem solution.

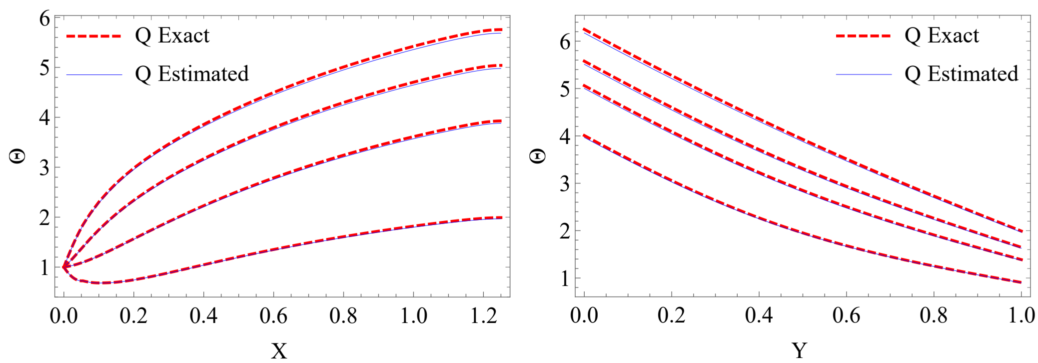

Figure 4. Comparison of the solutions of the forward problem, model $\mathcal{M}_0$

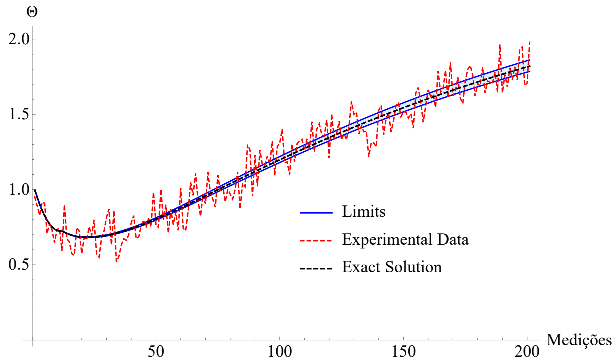

Figure 5. credibility gap, model $\mathcal{M}_0$

3.2 Case 2A

In this case, the heat flux $Q(x)$ has a linear dependence on the position along the length of the microchannel. The goal, then, is to estimate the parameters that constitute this functional behavior (slope and intercept of the line). The prior probability densities were adopted as $b \sim \mathcal{U}[-10, 10]$, $c \sim \mathcal{U}[-10, 10]$. Figure 6 shows the histogram of the posterior density of the samples for the parameters of the model $\mathcal{M}_1$.

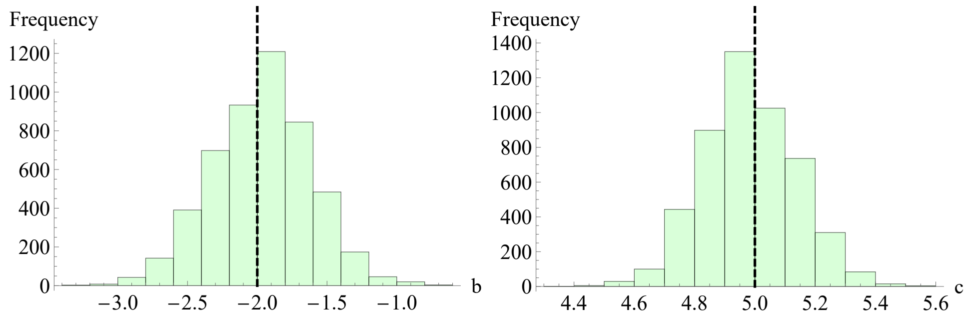

Figure 6. Histogram of the posterior distribution, model $\mathcal{M}_1$

Table 4 displays the inferred statistical data about the estimated parameters for model $\mathcal{M}_1$.

Table 4. Statistical inferences of Q, model $\mathcal{M}_1$

Parameter	**Exact Value**	**Mean**	**Standard Deviation**
b	-2.0	-1.96835	0.35457
c	5.0	4.98225	0.15407

It can be observed that the means of the samples from the posterior density approach the reference values used in the generation of experimental data, with low standard deviation. This demonstrates the method's ability to accurately estimate multiple parameters simultaneously.

Figure 7 shows the comparison between the exact function representing $Q(x)$ for model $\mathcal{M}_1$ and the function composed of the estimated parameters in the inverse problem.

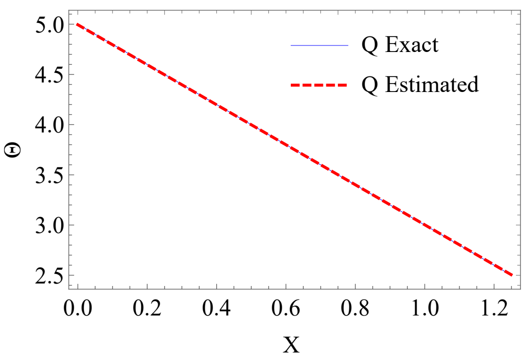

Figure 7. Estimated function, model $\mathcal{M}_1$

The forward problem was then solved again with the estimated function found in the inverse problem. Figure 8 shows the comparison of solutions with the exact $Q(x)$ and the estimated $Q(x)$ along L in the X direction as well as in the Y direction. Figure 9 shows the 95% credibility gap of the parameters for casa 2A.

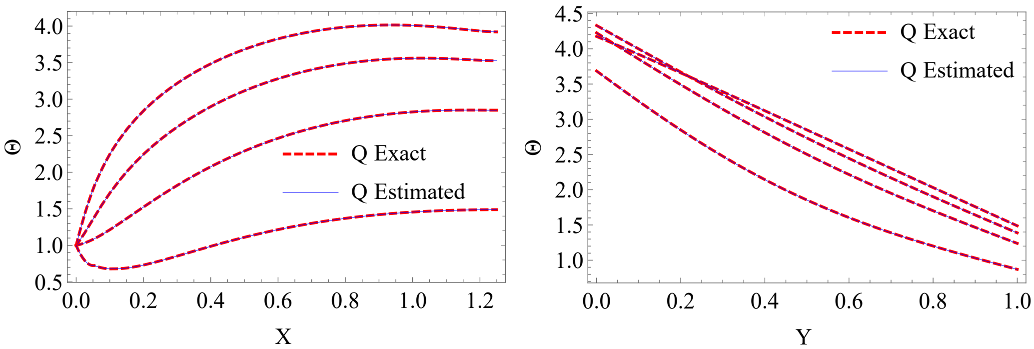

Figure 8. Comparison of the solutions of the forward problem, model $\mathcal{M}_1$

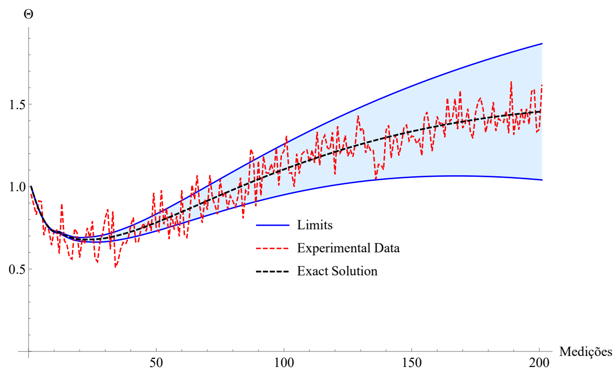

Figure 9. credibility gap; $\mathcal{M}_1$

In this case, the credibility interval is larger, as the uncertainty regarding the parameters also increases (larger standard deviation, an increase in the number of parameters to be estimated, and variation of the value with position). Therefore, the interval encompasses both the reference response of the problem, as well as the majority of the simulated experimental data.

3.3 Case 3A

In this case, $Q(x)$ has a quadratic dependence with the position along the length of the microchannel and the prior probability densities were adopted as $a \sim \mathcal{U}[-20, 15]$, $b \sim \mathcal{U}[-20, 15]$ and $c \sim \mathcal{U}[-20, 15]$. Figure 10 shows the histogram of the posterior density of the samples for the parameters of the model $\mathcal{M}_2$.

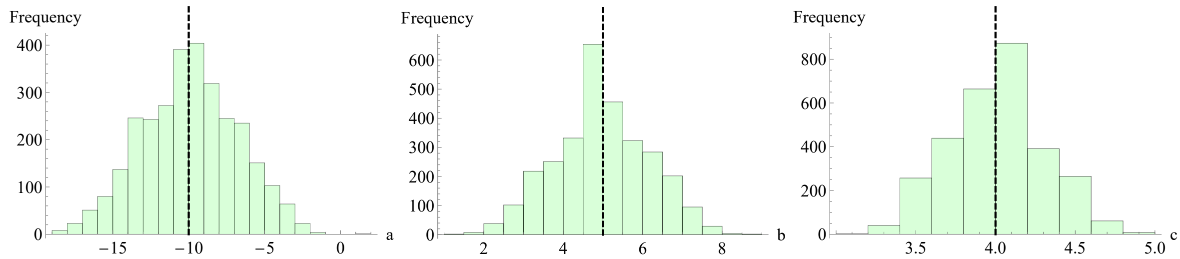

Figure 10. Histogram of the posterior distribution, model $\mathcal{M}_2$

Table 5 displays the inferred statistical data about the estimated parameters for model $\mathcal{M}_2$.

Once again, the algorithm was able to estimate the values of the uncertain parameter vector θ with satisfactory accuracy, with means very close to the reference values. In this case, however, a higher standard deviation can be observed concerning the parameters, especially in a, which is associated with the quadratic term of the function.

Figure 11 shows the comparison between the exact function representing $Q(x)$ for model $\mathcal{M}_1$ and the function composed of the estimated parameters in the inverse problem.

Table 5. Statistical inferences of Q, model model $\mathcal{M}_2$

Parameter	**Exact Value**	**Mean**	**Standard Deviation**
a	-10.0	-9.90393	3.1681
b	5.0	4.96772	1.18812
c	4.0	4.00427	0.298405

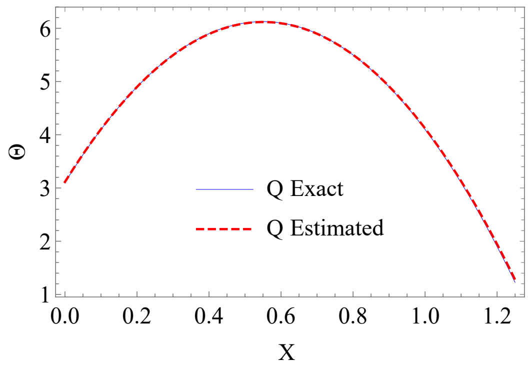

Figure 11. credibility gap, model $\mathcal{M}_2$

The forward problem was then solved again with the estimated function found in the inverse problem. Figure 12 shows the comparison of solutions with the exact $Q(x)$ and the estimated $Q(x)$ along L in the X direction as well as in the Y direction. Figure 13 shows the 95% credibility gap of the parameters for casa 2A.

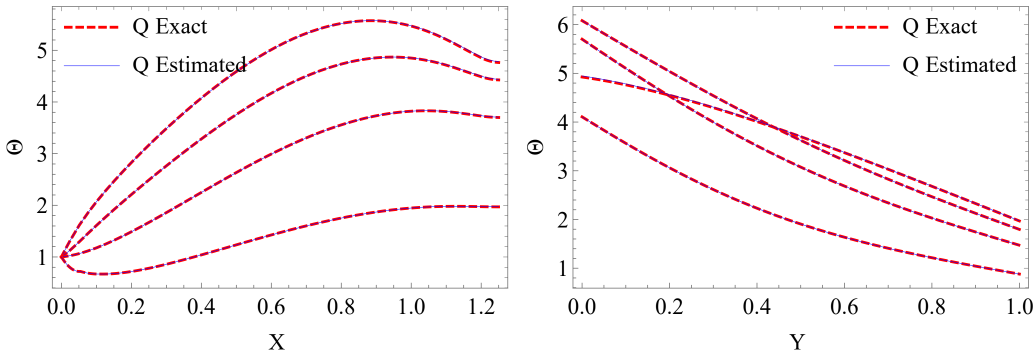

Figure 12. Comparison of the solutions of the forward problem, model $\mathcal{M}_2$

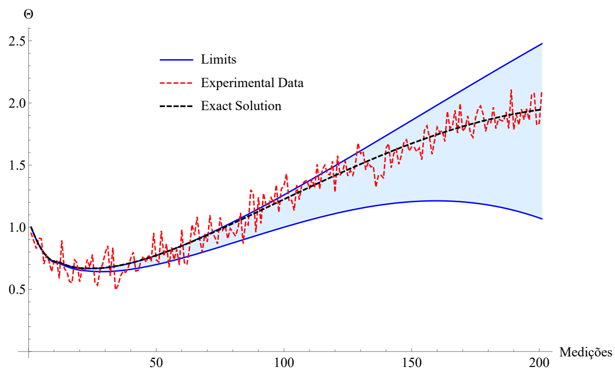

Figure 13. credibility gap; $\mathcal{M}_2$

Here, the credibility interval is also larger due to the greater uncertainty associated with the uncertain parameters, but the solution still accurately represents the behavior of the system, as it encompasses both the reference response and the simulated experimental data.

4. CONCLUSION

Based on the presented results, we can conclude that the Transitional Markov Chain Monte Carlo Method was effective in estimating all the proposed models for a heat flux imposed on one of the boundaries of a convective heat transfer problem in microchannels. Polynomial functionals were introduced, but the method can be extrapolated to a wide range of functional behaviors that make sense physically. As a next step, the intention is to incorporate information regarding model selection, which is one of the major advantages of the inversion method employed.

5. ACKNOWLEDGEMENTS

This study was financed in part by the Coordenação de Aperfeiçoamento de Pessoal de Nível Superior - Brasil (CAPES) Finance Code 001.

6. REFERENCES

Betz, W., Papaioannou, I. and Straub, D., 2016. "Transitional markov chain monte carlo: observations and improvements". *Journal of Engineering Mechanics*, Vol. 142, No. 5, p. 04016016.

Chen, K., Cotta, R.M., Naveira-Cotta, C.P. and Pontes, P.C., 2022. "Heat transfer analysis of compressible laminar flow in a parallel-plates channel via integral transforms". *International Communications in Heat and Mass Transfer*, Vol. 138, p. 106368.

Ching, J. and Chen, Y.C., 2007. "Transitional markov chain monte carlo method for bayesian model updating, model class selection, and model averaging". *Journal of engineering mechanics*, Vol. 133, No. 7, pp. 816–832.

Cotta, R.M., Knupp, D.C. and Naveira-Cotta, C.P., 2016. *Analytical heat and fluid flow in microchannels and microsystems*, Vol. 164. Springer.

Kaipio, J. and Somersalo, E., 2006. *Statistical and computational inverse problems*, Vol. 160. Springer Science & Business Media.

Kandlikar, S., Garimella, S., Li, D., Colin, S. and King, M.R., 2005. *Heat transfer and fluid flow in minichannels and microchannels*. elsevier.

Mercone, S., Frésard, R., Caignaert, V., Martin, C., Saurel, D., Simon, C., André, G., Monod, P. and Fauth, F., 2005. "Nonlinear effects and joule heating in i-v curves in manganites". *Journal of applied physics*, Vol. 98, No. 2, p. 023911.

Naveira-Cotta, C.P., Cotta, R.M. and Orlande, H.R., 2010. "Inverse analysis of forced convection in micro-channels with slip flow via integral transforms and bayesian inference". *International journal of thermal sciences*, Vol. 49, No. 6, pp. 879–888.

Orlande, H.R., 2015. "The use of techniques within the bayesian framework of statistics for the solution of inverse problems". *Metti 6 Advanced School: Thermal Measurements and Inverse Techniques*.

Ozisik, M.N. and Orlande, H.R., 2021. *Inverse heat transfer: fundamentals and applications*. CRC press.

Tuckerman, D.B. and Pease, R.F.W., 1981. "High-performance heat sinking for vlsi". *IEEE Electron device letters*, Vol. 2, No. 5, pp. 126–129.

Yarin, L., Mosyak, A. and Hetsroni, G., 2009. "Velocity field and pressure drop in single-phase flows". *Fluid Flow, Heat Transfer and Boiling in Micro-Channels*, pp. 103–144.

7. RESPONSIBILITY NOTICE